Published in final edited form as:
J Immunol. 2009 September 15; 183(6): 4055–4066. doi:10.4049/jimmunol.0900593.

Site-specific CPB1 tyrosine nitration and patho-physiological implications following its physical association with NOS-3 in experimental sepsis

Saurabh Chatterjee[*,†], **Olivier Lardinois**[†], **Marcelo G. Bonini**[†], **Suchandra Bhattacharjee**[†], **Krisztian Stadler**[†], **Jean Corbett**[†], **Leesa J. Deterding**[‡], **Kenneth B. Tomer**[‡], **Maria Kadiiska**[†], and **Ronald P. Mason**[†]

[†]Free Radical Metabolism Group, Laboratory of Pharmacology, NIEHS, Research Triangle Park, NC27709, USA

[‡]Laboratory of Structural Biology, NIEHS, Research Triangle Park, NC27709, USA

Abstract

Lipopolysaccharide (LPS)-induced sepsis results in oxidative modification and inactivation of carboxypeptidase B1 (CPB1). Here, immunoprecipitated CPB1 was probed for tyrosine nitration using monoclonal nitrotyrosine-specific antibodies in a murine model of LPS-induced sepsis. Tyrosine nitration of CPB1 was significantly reduced in the presence of NOS inhibitors, and xanthine oxidase (XO) inhibitor allopurinol and NOS-3 KO mice. CPB1 tyrosine nitration and loss of activity by the concerted action of NOS-3 and XO were also confirmed *in vitro* using both the nitric oxide donor 3-morpholinosydnonimine (SIN-1) and peroxynitrite. LC/MS/MS data indicated five sites of tyrosine nitration *in vitro* including Tyr-248, the tyrosine at the catalytic site. The site and protein specific nitration of CPB1 and the possible high nitration yield to inactivate it were elucidated by confocal microscopy. The studies indicated that CPB1 co-localized with NOS-3 in the cytosol of sinus lining cells in the red pulp of the spleen. Further analysis of CPB1-immunoprecipitated samples indicated immunoreactivity to a monoclonal NOS-3 antibody, suggesting protein complex formation with CPB1. XO, NOS inhibitors and NOS-3 KO mice injected LPS had decreased levels of C5a in spleens of septic mice, indicating peroxynitrite as a possible cause for CPB1 functional alteration. Thus, CPB1 co-localization, coupling, and proximity to NOS-3 in the sinus lining cells of spleen red pulp could explain the site-specific tyrosine nitration and inactivation of CPB1. These results open up new avenues for investigation of several enzymes involved in inflammation and their site-specific oxidative modifications by protein-protein interactions as well as their role in sepsis.

Keywords

oxidative-stress; sepsis; spleen; peroxynitrite; nitrotyrosine; Complement 5a

Introduction

The possible formation of peroxynitrite and the resultant post-translational nitration of protein tyrosine residues are associated with the pathogenesis of a series of diseases, including acute and chronic inflammatory processes, sepsis, ischemia-reperfusion and neurodegenerative

[*]**Author for correspondence:** Dr. Saurabh Chatterjee, Ph.D., Free Radical Metabolism Group, Laboratory of Pharmacology, National Institute of Environmental Health Sciences, National Institutes of Health, 111 T.W. Alexander Dr., Research Triangle Park, North Carolina 27709, USA. chatterjees2@niehs.nih.gov.

diseases (1,2**)**. Nitration of tyrosine residues by radical mechanisms is always tyrosyl- and nitric oxide- or nitrogen dioxide-dependent (3). Despite the number of diseases and pathological conditions in which tyrosine nitration has been observed, our knowledge of specific enzyme targets is limited, especially where a distinctive association is found between tyrosine nitration and functional alterations.

Tyrosine nitration does not depend on the abundance or number of tyrosine residues present on a particular protein (2). The commonalities among various nitrated proteins include glutamate or aspartate residues in the vicinity of Tyr residues and/or the presence of turn-inducing amino acids such as proline or glycine (4-6). Tyrosine nitration yields in proteins, organs and disease conditions have typically been low; the poor yield has raised questions about nitration as a post-translational modification in the molecular basis of disease (2).

Tissue carboxypeptidase B was initially described as a pancreatic metallocarboxypeptidase or CPB1 and is a marker for acute pancreatitis. This stable protease has high homology with plasma CPB and has substrates in common with it. This was assessed in recent studies where supplementation of the matrix with additional thrombin activatable fibrinolysis inhibitor (TAFI) or CPB produced a reduction in capillary tube formation (7). Plasma CPB or CPU or active TAFIa has a half- life of 8 minutes and plays a role in inflammation (8-10). Earlier work from this laboratory has identified CPB1 in the septic spleen and found it to form a radical in the presence of xanthine oxidase and NOS-3. This study further investigates the nature of the radical and its post translational modification.

In this work, we address the site-specific nature of protein tyrosyl radical formation and nitration and the higher nitration yield generated in carboxypeptidase B1 (CPB1), a zinc-containing tissue metalloprotein, following lipopolysaccharide (LPS)-induced systemic inflammation. Our previous work has shown that LPS-induced systemic inflammation leads to the formation of CPB1 radicals, which are mediated by xanthine oxidase and endothelial nitric oxide synthase (NOS-3) with a concomitant loss of enzyme activity (11). Immuno-spin trapping of the CPB1 radical was a significant step in the demonstration of the involvement of NOS-3- and XO-derived oxidizing species *in vivo*. However, molecular and post-translational footprints of reactive oxygen species (ROS)- and reactive nitrogen species (RNS)-based oxidative stress needed to be identified. We used relatively specific NOS inhibitors to identify the relative contributions of different NOS isoforms and peroxynitrite decomposition catalysts to identify the role of peroxynitrite in CPB1-tyrosine nitration. The CPB1 inhibitor DL-2-mercaptomethyl-3-guanidinoethylthiopropionic acid (MGTA) was used to study the involvement of the catalytic process in the nitration of CPB1.

Furthermore, to understand the molecular basis of CPB1, we have examined the role of SIN-1 and peroxynitrite in tyrosine oxidation and nitration *in vitro*. Importantly, it has been shown that carboxypeptidase M (CPM) cleaves peptides at crucial arginine residues and contributes to the arginine pool (12). We hypothesized that CPB1 sensitivity to nitration was due to its proximity to NOS-3 activated during inflammatory stress, providing it with a crucial substrate in inflammatory conditions. This hypothesis has now been supported by the co-localization of NOSs, xanthine oxidase, and CPB1 in the spleen. We also studied the enzyme inactivation of CPB1 and its correlation with nitrotyrosine formation and identified the sites of the tyrosine residues nitrated. We report the coupling of NOS-3 with CPB1, the formation of NO via NOS-3, and the role of XO in producing $O_2^{\bullet-}$, whose concerted action with NOS-3-derived NO leads to tyrosine nitration of CPB1. The above-mentioned events might result in higher nitration yields sufficient to inactivate CPB1 in sepsis.

Materials and Methods

Materials

LPS (*Escherichia coli*: Strain 55:B5), porcine carboxypeptidase B (CPB), 3-morpholinolsydnonimine hydrochloride (SIN-1) and allopurinol were obtained from Sigma Chemical Co. The spin trap 5,5-dimethyl-1-pyrroline *N*-oxide (DMPO) was obtained from Alexis Biochemicals. Trypsin (from bovine pancreas, modified, sequencing grade) and chymotrypsin (from bovine pancreas, modified, sequencing grade) were obtained from Roche Molecular Biochemicals. All other chemicals were of analytical grade and were purchased from Sigma Chemical Co. or Roche Molecular Biochemicals. All aqueous solutions were prepared using water passed through a Picopure 2UV Plus system (Hydro Services and Supplies, Inc. RTP, NC) equipped with a 0.2 μm pore size filter. Absorption spectra were recorded on a Cary 100 UV-visible spectrometer (Varian). High pressure liquid chromatography (HPLC) was carried out on an Agilent Chemstation (Agilent Technologies), 1100 liquid chromatography system equipped with a control module, binary pump, manual injector, and diode-array UV-vis detector. HPLC fractions were collected using a fraction collector, Model 2110 (Bio-Rad).

Mice

Adult male, pathogen-free, 8–10-week-old C57BL6/J mice (Jackson Laboratories) weighing 23–27 g on arrival were used in these experiments. The animals were housed for 1 week, one to a cage, before any experimental use. Experiments using mice that contained the disrupted NOS-2 (NOS-2$^{-/-}$, B6;129P2-*Nos2*^{tm1Lau}/J), gp91phox (gp91phox$^{-/-}$; B6.129S6-Cybb^{tm1Din}) and NOS-3 (NOS-3$^{-/-}$; B6.129P2-*Nos3*^{tm1Unc}/J backcrossed onto the C57BL6/J for twelve generations) genes were treated identically. The control animals for knockout experiments were age-matched mice of C57BL6/J origin in the case of NADPH oxidase and NOS-3 and B6129PF2/J in the case of NOS-2 that had normal NOS-2, NADPH oxidase, and NOS-3 activity. Mice had *ad libitum* access to food and water and were housed in a temperature-controlled room at 23–24 °C with a 12-hour light/dark schedule. All animals were treated in strict accordance with the NIH Guide for the Humane Care and Use of Laboratory Animals, and the experiments were approved by the institutional review board.

LPS-induced systemic inflammation model

Systemic inflammation was induced in mice following LPS administration as described previously (11,13). Briefly, mice received a bolus infusion of LPS (6 and 12 mg/ kg), (referred to as 0 h). A sham group was also included, where normal mice received saline in place of LPS. LPS was dissolved in pyrogen-free saline and administered through the intraperitoneal (i.p.) route. At +6 h, mice from the sham group and the LPS groups were sacrificed. The spleens were collected and snap-frozen in liquid nitrogen. Tissues were homogenized in phosphate buffer containing 100 μM DTPA and centrifuged at 3000 RPM at 4° C for 20 minutes. The samples were stored at −80° C until further use.

Administration of allopurinol, NOS inhibitors, CPB inhibitor, and peroxynitrite scavenger FeTPPS

Allopurinol, a specific inhibitor of xanthine oxidase (XO), the non-selective NOS-3 inhibitors N^5-(1-Imino-3-butenyl)-L-ornithine (L-NIO), Vinyl-L-NIO (Cayman Chemical), putatively selective inhibitor of neuronal nitric oxide synthase (nNOS) 1-(2-trifluoromethylphenyl) imidazole (TRIM) (Calbiochem) and the NOS-2 inhibitor N-3-(aminomethyl) benzylacetamide·2HCL (1400W, Sigma Chemical Co.) were administered in a single bolus dose of 20 mg/kg through the intra-peritoneal (i.p.) route 30 minutes prior to LPS treatment. In different experiments, the peroxynitrite decomposition catalyst 5,10,15,20-tetrakis(4-

sulfonatophenyl)pophyrinato iron III chloride (FeTPPs, Calbiochem) and the CPB-1 inhibitor DL-2-mercaptomethyl-3-guanidinoethylthiopropionic acid (MGTA, Sigma Chemical Co.), an inhibitor of carboxypeptidase B, were administered as bolus doses (30 and 100 mg/kg) and (20 mg/kg), respectively, through the i.p. route 15 minutes prior to LPS administration.

Immunoprecipitation and immunoblotting

CPB1 was immunoprecipitated with polyclonal anti-CPB1 antibody (R & D Systems) using the Seize X Mammalian Immunoprecipitation Kit (Pierce Biomedical) with some modifications. Solubilized spleen cell homogenates adjusted to a protein concentration of 150 μg per sample were pre-cleared by adding 200 μl of ProteinA/G-agarose followed by incubation for 1 h at room temperature. The homogenate was then incubated overnight with 30 μl of polyclonal anti-mouse CPB1 antibody (0.1 μg/μl) and the antigen-antibody mixture further incubated with the ProteinA/G-agarose slurry overnight. Immune complexes were eluted with elution buffer according to the manufacturer's instructions. Anti-CPB-1 immunoprecipitates were subjected to SDS/PAGE on 4–12% Bis Tris gels (Invitrogen) and electroblotted onto nitrocellulose membranes. Antibodies for the corresponding western blots used in these experiments were mouse monoclonal anti-nitrotyrosine (1:1000 dilution; Abcam). In some experiments, lysates were subjected to immunoblotting without immunoprecipitation. Antibodies used in these experiments were anti-mouse polyclonal CPB-1 (1:1000 dilution, R&D Systems), mouse monoclonal anti-NOS-3 (1:1000; Cell Signaling) and purified rat anti-mouse C5a (1:2000, BD Pharmingen). The immunocomplexed membranes were probed (1h at RT) with either goat anti-rabbit (1:5000, Upstate Biotechnologies), donkey anti-goat (1:3000,R&D Systems) or goat anti-mouse (1:5000, Pierce) horseradish peroxidase-conjugated secondary antibodies. Immunoreactive proteins were detected using enhanced chemiluminescence (Immobilon ™ Western Chemiluminiscence HRP substrate, Millipore). The images were subjected to densitometry analysis using LabImage 2006 Professional™ 1D gel analysis software from KAPLEAN Bioimaging Solutions.

Carboxypeptidase activity assay

Carboxypeptidase activity of immunoprecipitates was measured using the Actichrome TAFI Activity Kit (American Diagnostica, Inc.) according to the procedure described by the manufacturer with some modifications. Briefly, the reaction was initiated by adding 50 μl of TAFI substrate to 25 μl of anti-CPB-1 immunoprecipitates. After incubation for 30 minutes at 37 °C, the reaction was stopped by the addition of sulfuric acid, and the released chromogenic product was measured at 490 nm. The A_{490} of blanks, which consisted of complete mixtures incubated for 0 min, was subtracted from each value. CPB concentration in immunoprecipitates was estimated by ELISA using anti-CPB-1 antibody (1:1000, R&D Systems). A calibration curve was constructed with known concentrations of recombinant mouse CPB1 (R&D Systems).

The activity of purified porcine CPB was estimated by monitoring the formation of hippuric acid liberated from hippuryl-L-arginine (14,15). Formation of hippuric acid was monitored at 254 nm under the following assay conditions: 1 mM hippuryl-L-arginine, 4 nM CPB, 100 mM NaCl, 25 mM Tris-HCl, pH 7.65 at 25 °C. The concentration of purified porcine CPB solutions was determined at 278 nm ($\varepsilon = 7.35 \times 10^4\ M^{-1}cm^{-1}$) (14).

Confocal microscopy

For confocal studies, C57BL/B6 wild-type mice were injected with LPS, 12 mg/kg, and sacrificed at 6 h post LPS administration. Spleens were collected and washed in PBS and the tissues fixed in 10% neutral buffered formalin. After fixation, spleens were removed and placed in 30% sucrose for 24 h. Tissues were then sliced on a microtome into 20-μm sections, placed in PBS, and then permeabilized with 0.1% Surfact-Amps-X-100 (Pierce Biomedical) for 1 h.

After blocking with 0.1% BSA in PBS, NOS-3 was stained using monoclonal anti-NOS-3 antibody (BD Transduction Laboratories) as the primary antibody and Alexafluor 488 anti-mouse conjugated with fluorescein (Molecular Probes-Invitrogen) as the secondary antibody. CPB1 localization was probed by incubating the same slides with anti-CPB1 polyclonal antibody and Alexafluor 594 anti-goat secondary antibody. Secondary controls were used to determine background fluorescence by applying the secondary antibody only (data not shown). Slices were mounted on microscope cover glasses (22 × 22 mm, 1 mm thickness) (Erie Scientific, Portsmouth, NH) and sections analyzed under a confocal laser microscope (Zeiss).

C5a chemotaxis assay

Cell migration assay was carried out using the CytoSelectTM 96 well cell migration assay kit (Cell Biolabs, Inc) following the manufacturer's protocol. HL-60 cells were used for the assay. Mouse recombinant C5a (R&D Chemicals) was used as a positive control and incubated in the feeder layer. A group where no rC5a was added served as the negative control.

Experiments with pancreatic CPB, mouse recombinant CPB1 (rCPB 1) peroxynitrite, and SIN-1 *in vitro*

To illustrate the possible post-translational modification of CPB *in vitro*, porcine CPB was incubated with different concentrations of SIN-1 and peroxynitrite in the presence or absence of 25 mM sodium bicarbonate. Peroxynitrite was prepared in the laboratory according to the method described by Bonini et al., (16,17). 100 μM of the CPB was dissolved in phosphate buffer, pH 7.4, and incubated with 300, 1250 or 2500 μM peroxynitrite or peroxynitrite donor SIN-1. In experiments with mouse recombinant CPB, 1 μM of mrCPB1 was dissolved in phosphate buffer, pH 7.4, and incubated with 3, 12.5 or 25 μM peroxynitrite. Samples consisting of only enzyme, only peroxynitrite or only SIN-1 formed the negative controls. The reaction mixture was incubated at 37 ° C for 1 h. The resultant reaction mixture was then separated by SDS-PAGE and tested for nitrotyrosine immunoreactivity by western analysis.

Sample preparation and proteolytic digestion

Typically, incubations contained 100 μM CPB in 50 mM potassium phosphate buffer, pH 7.4, and were carried out at 37 °C in the presence or absence of 25 mM sodium bicarbonate, as indicated in the figure legends. The reactions were initiated by the addition of different concentrations of peroxynitrite (3 to 25 eqs) and allowed to proceed for 30 min, after which the solutions were passed over a Sephadex G-25 gel filtration column (GE Healthcare Bio-Sciences) previously equilibrated and eluted with 100 mM Tris-HCl, pH 8.5. The samples were denatured with 6 M guanidine hydrochloride in 100 mM Tris-HCl, pH 8.5, at 60 °C for 30 min, reduced with 5 mM dithiothreitol at 37 °C for 30 min, and alkylated with 25 mM iodoacetamide at 37 °C for 30 min. The resulting solutions were then loaded onto a previously equilibrated PD-10 gel filtration column and eluted with 100 mM Tris-HCl, pH 8.5. After passage through the PD-10 column, carboxyamidated samples were digested using a 20:1 substrate-to-protease ratio for 16 h at 37 °C (trypsin) or for 16 h at 25 °C (chymotrypsin). Reactions were stopped by injecting the final mixture directly onto a reverse phase HPLC column.

Reverse phase HPLC analysis of proteolytic hydrolysates

Digested samples (200 μL) were injected directly onto a Vydac 218TP54, 4.6 mm × 250 mm, C18 reverse phase HPLC column. Peptides were eluted at a flow rate of 0.8 mL/min with a linear gradient from 100% solvent A (0.1% trifluoroacetic acid in water) to 50 % solvent B (0.085% trifluoroacetic acid in acetonitrile) over 80 minutes. A rapid gradient to 90% solvent B and then back to 100% solvent A was used to regenerate the column. The eluent was monitored at 214, 280 and 365 nm with an Agilent HP1100 diode array detector. HPLC fractions were collected with a fraction collector, and the fractions containing nitrated peptides

(as judged by the appearance of chromatographic peaks at 365 nm) were pooled, lyophilized, and stored at −70 °C for subsequent analysis.

Electrospray mass spectrometry

A Micromass Q-TOF Micro (Waters Micromass Corporation) hybrid tandem mass spectrometer was used for the acquisition of the electrospray ionization (ESI) mass spectra and tandem mass spectra. All experiments were performed in the positive ion mode. Lyophilized HPLC fractions of nitrated peptides were resuspended in a minimal volume (~50 μL) of 50:50 water:acetonitrile containing 0.1% formic acid and infused into the mass spectrometer at ~300 nL/min using a pressure injection vessel (18). The needle voltage was ~3,200 V and the collision energy was 10 eV for the MS analyses. Collision-induced dissociation experiments employed argon with collision energy between 30 and 50 eV. Data analysis was accomplished with a MassLynx data system and MaxEnt deconvolution software supplied by the manufacturer.

Statistical analyses

All *in vivo* experiments were repeated three times with 3 mice per group (N=3). All *in vitro* experiments were repeated three times and the statistical analysis was carried out using the Microcal Origin software package. Quantitative data from western blots as depicted from the relative intensity of the bands were analyzed by performing a one-tailed Student's *t* test. $P<0.05$ was considered statistically significant.

Results

LPS-induced septic shock produces CPB1 tyrosine nitration *in vivo*

CPB1 forms a DMPO-trappable protein radical in response to LPS treatment as detected by immuno-spin trapping (11). In order to detect whether the CPB1 radical was correlated with nitration of tyrosine residues, which is dependant on tyrosyl radical formation (19), spleen homogenates from sham and LPS (6 and 12 mg/kg) treatments were probed for 3-nitrotyrosine immunoreactivity (data not shown). The data shows anti-nitrotyrosine immunoblotting of spleen tissue homogenates from control and LPS-treated mice. A number of proteins showed detectable immunoreactivity towards the antibody at 6 h, but not in 3 or 24 h, in both the control and LPS-treated mice. The most prominently nitrated protein had a molecular weight of about 47 kDa. MALDI-TOF analysis of this 47 kDa band performed in an earlier study (11) resulted in the detection of more than ten proteins, one of which was carboxypeptidase B1 (CPB1).

To determine whether the CPB1 protein was nitrated, mouse spleen tissue lysates were immunoprecipitated with anti-CPB1 antibody. The immunoprecipitates were then immunoblotted with anti-nitrotyrosine antibody. Western blot analysis of the immunoprecipitates (Fig. 1A) indicated the presence of only one nitrated protein band of approximately 47 kDa. The results also indicated that CPB1 nitration was significantly higher in the LPS-treated group than the sham-treated group at 6h (Fig.1B). This result suggests that the 47 kDa-nitrated protein detected in the splenocyte lysate is indeed CPB1. As an additional control of specificity for nitration of CPB1, anti-CPB1 antiserum was pre-absorbed with mouse recombinant CPB1. The pre-absorbed antibody was used for immunoprecipitation of CPB1. Anti-CPB1 antibody was also pre-absorbed with bovine serum albumin (BSA) and normal rabbit serum (NRS) for negative controls.

Results indicated that immunoprecipitation of CPB1 using a CPB1 antibody pre-absorbed with mouse recombinant CPB1 had little or no reactivity to anti-nitrotyrosine antibody (Fig.1C, lanes 2 and 4), whereas immunoprecipitation of CPB1 using an antibody pre-absorbed with either BSA or NRS showed distinct bands on the western blot (Fig. 1C, lanes 1 and 3).

Tyrosine nitration of CPB1 is apparently due to formation of peroxynitrite and is mediated by xanthine oxidase and NOS-3

It is known that protein tyrosine nitration can be mediated by peroxynitrite (1). Superoxide and NO in a diffusion-controlled reaction yield peroxynitrite which, in biological systems, promptly reacts with carbon dioxide, leading to the formation of carbonate ($CO_3^{\bullet-}$) and nitrogen dioxide ($NO_2^{\bullet-}$) radicals (16,20,21,22). Although there are no direct methods to detect peroxynitrite *in vivo*, there are reports of certain classes of iron porphyrins which act as peroxynitrite decomposition catalysts (23).

To determine whether peroxynitrite plays a role in LPS-induced tyrosine nitration of CPB1, we treated mice with FeTPPS, a porphyrin peroxynitrite scavenger, prior to LPS treatment. Proteins from spleen homogenates were immunoprecipitated with anti-CPB1 and analyzed by western blotting using anti-nitrotyrosine. As depicted in Fig. 2A, administration of FeTPPS significantly inhibited the nitration of the protein, supporting the involvement of peroxynitrite.

Peroxynitrite is a powerful oxidant that is formed by the diffusion-limited reaction between nitrogen monoxide ($NO^{\bullet}$) and superoxide ($O_2^{-\bullet}$). To identify the possible $O_2^{\bullet-}$ and $NO^{\bullet}$ generators in LPS-treated mice, we used allopurinol, a specific XO inhibitor, 1400 W, a specific inhibitor for NOS-2, TRIM, a putatively specific inhibitor for NOS-1, and Vinyl-L-NIO and L-NIO, two nonselective inhibitors of all NOS isoforms. As seen in Fig. 2B, administration of the XO inhibitor allopurinol and two non-selective inhibitors of NOS isoforms L-NIO and Vinyl-L-NIO significantly inhibited the nitration of CPB1(Fig. 2B and 2C), while administration of 1400W, a specific inhibitor for NOS-2, and TRIM, a relatively specific inhibitor for NOS-1, did not inhibit nitration (Fig. 2D and 2E). Because the inhibitors showing marked isoform selectivity toward NOS-1 and NOS-2 did not inhibit the nitration of CPB1, whereas, in strong contrast, the nonselective inhibitors were highly effective, it is thus reasonable to suspect that NOS-3 plays a central role in the nitration process.

In the septic spleen, NOS-2 has been shown to be a major source of NO while at early sepsis (4–6h post LPS administration) NOS-3 and XO were major sources of $NO^{\bullet}$ and $O_2^{\bullet-}$ respectively (11,24). The respective roles of the three enzymes in the CPB1 nitration process were delineated using gene knockout (KO) mice. Western blot analysis of anti-CPB1 immunoprecipitates indicated that nitration of tyrosine residues was not blocked in either NOS-2 knockout mice (Fig. 2F and 2G, lane 4) or NADPH oxidase knockout mice (data not shown). In contrast no staining was observed for either sham or LPS treated NOS-3 KO mice (Fig. 2F and 2G, Lanes 2 and 3). These data indicate that NOS-3 is the primary NOS isoform responsible for CPB1 nitration *in vivo*.

To investigate the involvement of CPB1 in the catalysis of its self- nitration *in vivo*, we used MGTA, an inhibitor of CPB1, which binds to the catalytic site of the enzyme. Tyrosine nitration of immunoprecipitated CPB1 was completely blocked by the administration of this inhibitor in LPS-treated mice as shown in Fig. 2H and 2I.

LPS-induced peroxynitrite formation and nitration lead to inactivation of CPB1 *in vivo* and *in vitro*

In order to study the biological consequences of CPB1 tyrosine nitration, we measured the enzyme activity of CPB1. The activity index of immunoprecipitated CPB1 in LPS-treated mice and LPS+1400W-treated mice was significantly lower than in the sham treatment ($P<0.05$) (Fig.3A). Administration of allopurinol, L-NIO, or Vinyl-L-NIO to LPS-treated mice significantly increased the activity compared to the LPS-treated group alone ($P<0.05$). LPS-treated mice lacking the NOS-3 gene also had activity comparable to corresponding sham-treated NOS-3 KO mice (Fig. 3A). The results obtained *in vivo* were further confirmed with

parallel measurements of peroxynitrite-mediated nitration of CPB *in vitro* and loss of activity. When porcine CPB and/or mouse recombinant CPB1 (mrCPB1) was treated with 3, 6, 12.5, or 25 molar equivalents of peroxynitrite, there was a concentration-dependent increase in tyrosine nitration (Fig. 3 B, C, E, and F). The increased tyrosine nitration was associated with parallel decreases in activity of CPB, with more than 50% loss of activity with 12.5 molar equivalents of peroxynitrite (Fig. 3D).

LPS-induced tyrosine nitration of CPB1 and inactivation are linked to co-localization and protein complex formation with NOS-3

The loss of CPB activity in the presence of authentic peroxynitrite *in vitro* (50% activity loss with 12.5 equivalents or 1.25 mM peroxynitrite) raises the question of the possible existence of such concentrations of peroxynitrite in inflammatory physiology. Typically, protein tyrosine nitration is a relatively widespread *in vivo* modification, with its overall yield (expressed as moles of 3-nitrotyrosine/mole of tyrosine) being typically low. The low yield poses serious doubts about whether these modifications are relevant to the molecular basis of disease in patho-physiological states (2). In order to establish the connection between the inactivation of CPB1 *in vivo* and the concentration of peroxynitrite required to inactivate CPB *in vitro*, we sought to determine the localization of CPB1 in the spleen. We propose that a close proximity to the availability of NO and $O_2^{\bullet-}$ sources can create sufficiently high nitration yields in a site-specific manner so as to inactivate the enzyme. It has been shown that NO production in rat lung microvascular endothelial cells (RLMVEC) is stimulated more efficiently by arginine released from carboxypeptidase substrates than free arginine after LPS stimulation, thus indicating a mechanism by which the arginine supply for NO production in inflammatory conditions may be maintained (12).

These observations prompted us to investigate whether subcellular co-localization of two enzymes in the splenic vascular bed resulted in a steady flow of NO and formation of higher concentrations of peroxynitrite. This could lead to high nitration yields that are not obtained even in inflammatory microenvironments where the enzymes are widely separated. Confocal microscopy results indicated that both levels of CPB1 and NOS-3 were high in the septic spleen and that CPB1 co-localized with NOS-3 in the sinus lining cells of the red pulp. NOS-3 was mostly localized in the membrane in sham-treated spleens (Fig. 4A:I), and LPS treatment resulted in translocation of NOS-3 to the cytosol and co-localization with CPB1 (Fig. 4A:II) (25). Cells lining the venous sinusoids also showed significant co-localization of CPB1 and NOS-3 (Fig. 4A:III). We did not observe the same co-localization pattern in the white pulp of the spleen (data not shown).

To further address whether the co-localization resulted from binding of CPB1 to NOS-3 following its activation and translocation into the cytosol in LPS- treated mice, immunoprecipitates with CPB1 were probed with monoclonal anti-NOS-3 antibody. In both the sham-treated and LPS-treated groups, there was an immunoreactive band at 140 kD corresponding to NOS-3, while in the NOS-3 KO group, no immunoreactivity was observed (Fig. 4B). The intensity of the bands was analyzed by band analysis software, and the band intensity from the LPS-treated group was significantly higher than in the sham-treated group (data not shown). These data strongly suggest that CPB1 existed in a form bound with NOS-3 in the sham- and LPS-treated spleens, but not in NOS-3 knockout mice (Fig. 4B).

CPB1 oxidative inactivation leads to accumulation of C5a in the LPS-treated spleen

It has recently been shown that thrombin-activatable CPB is catalytically more efficient than plasma carboxypeptidase N (CPN), the major plasma anaphylatoxin inhibitor, in inhibiting bradykinin, activated complement C3a, C5a, and thrombin-cleaved osteopontin *in vitro* (26). CPB inactivates these active inflammatory mediators by specific cleavage of the carboxyl

terminal arginines (10). Similarly, proCPB-deficient mice displayed enhanced pulmonary inflammation in a C5a-induced alveolitis (10). Based on the above evidence, we chose to probe the functional consequences of LPS treatment in the spleen. When we separated spleen tissue homogenate proteins by SDS-PAGE and immunoblotted them against C5a antibody, we found that LPS-treated and LPS+1400W-treated mouse spleen tissue homogenates showed significant levels of C5a compared to no detectable levels in sham-treated spleens (Fig. 5A and 5B). Accumulation of C5a under these conditions would lead to severe inflammatory reactions as seen in sepsis and septic shock.

The XO inhibitor allopurinol and the NOS-3 inhibitors L-NIO and Vinyl-L-NIO, which significantly decreased tyrosine nitration of CPB1 in spleens of LPS-treated mice (Fig. 2B), also blocked the expression of C5a in the LPS-treated spleen (Fig. 5A and 5B). Furthermore, levels of C5a were significantly increased in NOS-3 knockout mice compared to the corresponding knockout sham treatment, but were significantly lower than in LPS-treated wild type mice (Fig. 5C and 5D).

Since polyclonal anti-serum cannot distinguish between C5a (74 amino acids) and that of C5a-des Arg (73 amino acids), Neutrophil chemotaxis assay was performed to evaluate concentrations of C5a relative to its less active (5%) desArg form (27,28). . In a first set of experiments, HL 60 cell chemotactic response to purified C5a was examined. Results indicated that at 2×10^{-9} M, mouse recombinant C5a could induce chemotaxis of HL60 cells, whereas preincubation of C5a with mouse rCPB1 (mrCPB1) reduced chemotactic response by up to 40% (Fig. 5E). Little chemotactic activity was detecteble in the absence of C5a. Further, when nitro-mrCPB1 was incubated with mrC5a, chemotaxis was comparable to the control/ unmodified C5a. In a second set of experiments, HL-60 cells' chemotactic response to immunoprecipitated C5a from spleen tissue homogenates was evaluated. These experiments were performed using equal amounts of immunoprecipitated C5a, as assessed by ELISA. The results indicated that the chemotactic response was significantly higher for samples from LPS and LPS+1400W-treated mice than that observed for sham, allopurinol, L-NIO, Vinyl-L-NIO and LPS KO mouse samples (Fig. 5F)

in vitro characterization of peroxynitrite-induced chemical modifications of CPB1

In order to study the molecular basis of tyrosine oxidation and nitration of CPB by peroxynitrite *in vitro*, porcine CPB (100 μM) was incubated with peroxynitrite (300 μM) in the presence or absence of 25 mM sodium bicarbonate. Carbonate radicals ($CO_3^{\bullet-}$) can be formed biologically by the decomposition of the peroxynitrite-carbon dioxide adduct ($ONOOCO_2^-$) or enzymatic activities, i.e., peroxidase activity of CuZnSOD and xanthine oxidase turnover in the presence of bicarbonate (29,30,31). Peroxynitrite-dependent tyrosine nitration is likely to occur through the initial reaction of peroxynitrite with carbon dioxide or metal centers, leading to secondary nitrating species (19,32). We found that a reaction mixture containing sodium bicarbonate as a bicarbonate source showed several immunoreactive bands when compared to samples incubated with only peroxynitrite. CPB (32, 35 kD) and mouse CPB1 (43, 48 kD) migrate as doublets on an SDS PAGE gel. Apart from the monomer (35 kD) and a slightly less intense band at 30–32 kD, another distinct band of approximately 70 kD was immunoreactive to an antibody specific to 3-nitrotyrosine (Fig. 6).

Following this observation, we used SDS PAGE to analyze a reaction mixture containing both peroxynitrite and SIN-1 as a potential mimetic of the $O_2^{\bullet-}$/NO generation. The analysis revealed the formation of dimers, characterized by the 70 kD Coomassie stained band, compared to none in a sample containing only CPB (Fig. 7A). The dimers were inhibited in a dose-dependent manner when incubated with 10 and 100 mM DMPO (Fig. 7A). It has been reported that formation of dimers is the result of dityrosine crosslinks, which form by the reaction of two tyrosyl radicals. Dityrosine crosslinks are considered to be stable markers for oxidative

modification of proteins (33). To identify the nature of the dimer, we measured the fluorescence of the intact protein containing the reaction mixture at 410 nm. The spectra showed a pattern that is distinct for dityrosine formation in samples incubated with SIN-1, but was absent in samples containing CPB alone (Fig. 7B). When the reaction mixture was digested with trypsin and run through a reverse phase HPLC column, a spectrum indicative of dityrosine crosslink formation was found in one of the peptides (data not shown).

Nitration of the catalytic site tyrosines (Tyrosine-248 and Tyrosine-198) as an index of tyrosine oxidation and inactivation of CPB

In order to examine the possible sites of tyrosine nitration of CPB, the enzyme was incubated with 12.5 molar equivalents of peroxynitrite, digested with either chymotrypsin or trypsin, and subjected to reverse phase HPLC. The fractions corresponding to the absorbance at 365 nm were collected and subjected to MS/MS analysis. At least eleven peptides with five sites of nitration on tyrosine residues were identified. These include Tyr-92, Tyr-210, Tyr-277, Tyr-248 and Tyr-198. Of these, Tyr-248 and Tyr-198 are located in the catalytic site of CPB (Table 1). The observed nitration of the Tyr-248 was consistent with previous findings that Tyr-248 is more reactive and undergoes nitration with an 8-fold molar excess of tetranitromethane (34).

Discussion

We have previously shown that CPB1 produces a DMPO-trappable protein radical *in vivo* in LPS-induced systemic inflammation and that this radical production is mediated by the dual role of NOS-3 and xanthine oxidase (11). In the present work, we report the site-specific nitration of splenic CPB1, possibly mediated by peroxynitrite, *in vivo* and *in vitro* in LPS-induced acute inflammation in mice, a model that resembles systemic inflammation response syndrome, or SIRS.

We chose to use FeTPPS, a relatively specific peroxynitrite decomposition catalyst *in vivo* (35), to investigate the involvement of peroxynitrite in CPB1 nitration. We limited our studies with FeTPPS *in vivo* to relating the tyrosine nitration process of CPB1 to peroxynitrite formation in LPS-induced systemic inflammation.

In peroxynitrite formation in sepsis, nitric oxide from NOS is known to play a very important role (36). Here, the involvement of NOS-3 as a principal source of peroxynitrite at 6 h was confirmed using both NOS-3 and NOS-2 knockout mice. NOS-2 knockout mice showed no significant difference in immunoreactivity to 3-nitrotyrosine antibody, suggesting the important role played by NOS-3 in peroxynitrite formation and nitration of CPB1.

Tyrosine nitration at catalytic sites has been shown to result in loss of activity in many enzyme targets (2). To determine whether the catalytic site tyrosines of CPB1 were targets of nitration *in vivo*, we blocked the catalytic site by administering MGTA, a specific inhibitor of carboxypeptidase B-like metalloproteases that binds efficiently to the catalytic site (12,37). Tyrosine nitration of CPB1 was completely blocked by MGTA (Fig. 2D). Carboxypeptidase B-like enzymes are known to contribute to the arginine pool by providing the substrate to NOSs (12). By binding to the catalytic site, MGTA decreased the production of arginine from peptide substrates and the production of NO. This effect might result in decreased peroxynitrite formation and complete inhibition of tyrosine nitration of CPB1. Also, blocking of tyrosine nitration of CPB1 after administration of MGTA would suggest that most of the target nitration sites may be located in the catalytic subunit of the enzyme, since MGTA binding would have masked the catalytic site tyrosines in CPB1. This evidence clearly pointed to the tyrosine nitration of CPB1 *in vivo*, but did not define the specificity of the nitration process in CPB1, a zinc-containing metalloprotein. Analysis of the results from experiments using porcine CPB

tissue (Table 1) clearly showed the existence of at least five sites of nitration on tyrosine residues.

There has been considerable speculation recently that protein tyrosine nitration is only a biomarker rather than an event that alters protein function. Our *in vitro* data with CPB and peroxynitrite suggests that nitration yields sufficient to cause <50% loss of activity require a 12.5 molar excess or 1.25 mM peroxynitrite (Fig 3B, right panel), while CPB1 loses >50% of its activity in pathophysiological conditions that mimic sepsis (Fig. 3). Porcine CPB was found to be nitrated at Tyr-248 with an 8-fold molar excess of tetranitromethane, with enzymatic activity towards both basic and non-basic substrates falling to less than 30% of the control (34). The relative yield of protein 3-NT formation, even for proteins considered to be preferential targets for nitration, is, in general, low. As a result, the biological relevance of protein tyrosine nitration has been questioned, mainly in the context of the loss of protein function (38). We attribute the loss of activity of CPB1 in the spleen to its proximal association and binding to NOS-3 in the early septic spleen. In order to define the specific nature of CPB1 nitration and inactivation *in vivo*, we chose to examine the proximal association and protein-protein coupling in a cellular compartment as a possible way to nitrate specific tyrosines with a high nitration yield. The results, which demonstrated the co-localization, co-translocation and coupling of CPB1 with NOS-3 (Fig. 4A and 4B), supported our assertion that CPB1 nitration is protein- and site-specific. Also, our data strongly suggest a novel argument that tyrosine nitration of CPB1 affects its physiological functions owing to its proximal association with NOS-3 in the sinus lining cells of the spleen.

The 3-nitrotyrosine moiety is often localized to specific tissue regions and cell types in different inflammatory disease processes, indicating a close association between sites of production of nitrating species and susceptible target proteins (39). Specific CPB1 tyrosine nitration and loss of activity in septic mice is presumably due to the higher nitration yield attained in the local microenvironment (Fig. 8). This possibility is supported by the fact that nitration was significantly decreased in the presence of allopurinol, a specific inhibitor of xanthine oxidase. Proximal association of CPB1 with NOS-3 and sufficient superoxide generation formed via xanthine oxidase could generate peroxynitrite, resulting in nitration of one or more tyrosine residues that are important for catalysis of CPB1 (Fig. 8).

LC/MS/MS analysis of nitro CPB showed five potential sites of nitration of tyrosine residues, including Tyr-248 and Tyr-198, which are located in proximity to the Zn atom in the catalytic site. A loss of function of CPB as observed with 12.5 molar equivalents or 1.25 mM peroxynitrite (Fig. 3B) could be attributed to the nitration of Tyr 248 and Tyr 198 (Table 1).

The significant inactivation of CPB1 *in vivo* was probed further for any functional alteration of the enzyme. The hydrolysis of peptide bonds at the C-terminus of peptides and proteins carried out by carboxypeptidases may be a step in the degradation of some substrate molecules or result in the maturation of others. The physiological effect of these enzymes, as for every type of protease, is thus varied and site- and organism-dependent (40). The presence of significantly increased levels of CPB1 has been identified in the spleens of septic mice (11). Since enzymes of the carboxypeptidase family, especially CPB2 or TAFI, have been known to cleave basic arginine and lysine residues from peptides like C5a and bradykinin and regulate inflammation (10), the functional significance of enzyme inactivation was probed in septic mice. The results of increased accumulation of C5a in LPS-administered mice (Fig. 5) and their regulation by NOS-3 and XO inhibitors may indicate a broader role for tyrosine nitration of CPB1.

In conclusion, we report the post-translational tyrosine nitration of CPB1 with significant loss of its activity and concomitant accumulation of C5a in the spleen. The pathological

consequences observed might be a result of high nitration rates due to the proximal association of CPB1 and NOS-3 in the sinus lining cells of the red pulp.

Acknowledgments

The authors sincerely acknowledge Tiwanda Marsh, Jeoffrey Hulbert and Jeff Tucker for excellent technical assistance. We also sincerely thank Dr. Ann Motten, Dr. Marilyn Ehrenshaft and Mary Mason for helping the careful editing of this manuscript.

Grant Support: This work has been supported by the Intramural Research Program of the National Institutes of Health and the National Institute of Environmental Health Sciences

REFERENCES

1. Radi R, Peluffo G, Alvarez MN, Naviliat M, Cayota A. Unraveling peroxynitrite formation in biological systems. Free Radical Biol. Med 2001;30:463–488. [PubMed: 11182518]
2. Souza JM, Peluffo G, Radi R. Protein tyrosine nitration - functional alteration or just a biomarker? Free Radical Biol. Med 2008;45:357–366. [PubMed: 18460345]
3. Nakai K, Kadiiska MB, Jiang J-J, Stadler K, Mason RP. Free radical production requires both inducible nitric oxide synthase and xanthine oxidase in LPS-treated skin. P. Natl. Acad. Sci. USA 2006;103:4616–4621.
4. Souza JM, Daikhin E, Yudkoff M, Raman CS, Ischiropoulos H. Factors determining the selectivity of protein tyrosine nitration. Arch. Biochem. Biophys 1999;371:169–178. [PubMed: 10545203]
5. Ischiropoulos H. Protein tyrosine nitration-An update. Arch Biochem Biophys 2009;484:117–21. [PubMed: 19007743]
6. Kanski J, Behring A, Pelling J, Schoneich C. Proteomic identification of 3-nitrotyrosine-containing rat cardiac proteins: effects of biological aging. Am. J. Physiol. Heart Circ. Physiol 2005;288:H371–H381. [PubMed: 15345482]
7. Guimarães AH, Laurens N, Weijers EM, Koolwijk P, van Hinsbergh VW, Rijken DC. TAFI and pancreatic carboxypeptidase B modulate in vitro capillary tube formation by human microvascular endothelial cells. Arterioscler. Thromb. Vasc. Biol 2007;7:2157–2162.
8. Bouma BN, Meijers JC. Thrombin-activatable fibrinolysis inhibitor (TAFI, plasma procarboxypeptidase B, procarboxypeptidase R, procarboxypeptidase U). J. Thromb. Haemost 2003;1:1566–1574. [PubMed: 12871292]
9. Arolas JL, Vendrell J, Aviles FX, Fricker LD. Metallocarboxypeptidases: emerging drug targets in biomedicine. Curr. Pharm. Des 2007;13:349–366. [PubMed: 17311554]
10. Leung LL, Myles T, Nishimura T, Song JJ, Robinson WH. Regulation of tissue inflammation by thrombin-activatavle carboxypeptidase B (or TAFI). Mol. Immunol 2008;45:4080–4083. [PubMed: 18706698]
11. Chatterjee S, Ehrenshaft M, Bhattacharjee S, Deterding LJ, Bonini MG, Corbett J, Kadiiska M, Tomer KB, Mason RP. Immuno- spin trapping of a post-translational carboxypeptidase B1 radical formed by a dual role of xanthine oxidase and endothelial nitric oxide synthase in acute septic mice. Free Radical Biol. Med 2009;46:454–461. [PubMed: 19049863]
12. Hadkar V, Sangsree S, Vogel SM, Brovkovych V, Skidgel RA. Carboxypeptidase-mediated enhancement of nitric oxide production in rat lungs and microvascular endothelial cells. Am. J. Physiol. Lung Cell Mol. Physiol 2004;287:L35–L45. [PubMed: 14977629]
13. Chatterjee S, Premachandran S, Shukla J, Poduval TB. Synergistic therapeutic potential of dexamethasone and L-arginine in lipopolysaccharide-induced septic shock. J. Surg. Res 2007;140:99–108. [PubMed: 17292408]
14. Folk JE, Wolff EC, Schirmer EW. The kinetics of carboxypeptidase B activity. II. Kinetics parameters of the cobalt and cadmium enzymes. J. Biol. Chem 1962;237:3100–3104. [PubMed: 13945772]
15. Folk JE, Piez KA, Carroll WR, Gladner JA. Carboxypeptidase B IV. Purification and characterization of the porcine enzyme. J. Biol. Chem 1960;235:2272–2277. [PubMed: 13823740]

16. Bonini MG, Radi R, Ferrer-Sueta G, Da AM, Ferreira C, Augusto O. Direct EPR detection of the carbonate radical anion produced from peroxynitrite and carbon dioxide. J. Biol. Chem 1999;274:10802–10806. [PubMed: 10196155]

17. Beckman JS, Beckman TW, Chen J, Marshall PA, Freeman BA. Apparent hydroxyl radical production by peroxynitrite: implications for endothelial injury from nitric oxide and superoxide. P. Natl. Acad. Sci. USA 1990;87:1620–1624.

18. Deterding LJ, Moseley MA, Tomer KB. Coaxial continuous flow fast atom bombardment in conjunction with tandem mass spectrometry for the analysis of biomolecules. Anal. Chem 1989;61:2504–2511. [PubMed: 2817405]

19. Nakai K, Mason RP. Immunochemical detection of nitric oxide and nitrogen dioxide trapping of the tyrosyl radical and the resulting nitrotyrosine in sperm whale myoglobin. Free Radical Biol. Med 2005;39:1050–1058. [PubMed: 16198232]

20. Meli R, Nauser T, Koppenol WH. Direct observation of intermediates in the reaction of peroxynitrite with carbon dioxide. Helv. Chem. Acta 1999;82:722–725.

21. Szabo C, Ischiropoulos H, Radi R. Peroxynitrite: biochemistry, pathophysiology and development of therapeutics. Nature reviews 2007;6:662–680.

22. Tortora V, Quijano C, Freeman B, Radi R, Castro L. Mitochondrial aconitase reaction with nitric oxide, S-nitrosoglutathione, and peroxynitrite: mechanisms and relative contributions to aconitase inactivation. Free Radical Biol. Med 2007;42:1075–1088. [PubMed: 17349934]

23. Imam SZ, El-Yazal J, Newport GD, Itzhak Y, Cadet JL, Slikker W Jr. Ali SF. Methamphetamine-induced dopaminergic neurotoxicity: role of peroxynitrite and neuroprotective role of antioxidants and peroxynitrite decompostition catalysts. Ann. NY Acad. Sci 2001;939:366–380. [PubMed: 11462792]

24. Kan W, Zhao KS, Jiang Y, Yan W, Huang Q, Wang J, Qin Q, Huang X, Wang S. Lung, spleen, and kidney are the major places for inducible nitric oxide synthase expression in endotoxic shock: role of p38 mitogen-activated protein kinase in signal transduction of inducible nitric oxide synthase expression. Shock 2004;21:281–287. [PubMed: 14770043]

25. Prakash P, Thatte HS, Goetz RM, Cho MR, Golan DE, Michel T. Receptor-regulated translocation of endothelial nitric-oxide synthase. J. Biol. Chem 1998;42:27383–27388.

26. Myles T, Nishimura T, Yun TH, Nagashima M, Morser J, Patterson AJ, Pearl RG, Leung LLK. Thrombin activatable fibrinolysis inhibitor, a potential regulator of vascular inflammation. J. Biol. Chem 2003;278:51059–51067. [PubMed: 14525995]

27. Fernandez HN, Henson PM, Otani A, Hugli TE. Chemotactic response to human C3a and C5a anaphylatoxins. I. Evaluation of C3a and C5a leukotaxis in vitro and under stimulated in vivo conditions. J. Immunol 1978;120:109–115. [PubMed: 342601]

28. Marder SR, Chenoweth DE, Goldstein IM, Perez HD. Chemotactic responses of human peripheral blood monocytes to the complement-derived peptides C5a and C5a des Arg. J. Immunol 1985;134:3325–3331. [PubMed: 3884709]

29. Augusto O, Bonini MG, Amanso AM, Linares E, Santos CCX, De Menezes SL. Nitrogen dioxide and carbonate radical anion: two emerging radicals in biology. Free Radical Biol. Med 2002;32:841–859. [PubMed: 11978486]

30. Zhang H, Joseph J, Gurney M, Becker D, Kalyanaraman B. Bicarbonate enhances peroxidase activity of Cu, Zn-superoxide dismutase. J. Biol. Chem 2002;277:1013–1020. [PubMed: 11682485]

31. Alvarez MN, Peluffo G, Folkes L, Wardman P, Radi R. Reaction of the carbonate radical with the spin-trap 5,5-dimethyl-1-pyrroline-*N*-oxide in chemical and cellular systems: pulse radiolysis, electron paramagnetic resonance, and kinetic-competition studies. Free Radical Biol. Med 2007;43:1523–1533. [PubMed: 17964423]

32. Alvarez B, Radi R. Peroxynitrite reactivity with amino acids and proteins. Amino Acids 2003;25:295–311. [PubMed: 14661092]

33. Heinecke JW, Li W, Daehnke HL III, Goldstein JA. Dityrosine, a specific marker of oxidation, is synthesized by the myeloperoxidase-hydrogen peroxide system of human neutrophils and macrophages. J. Biol. Chem 1993;268:4069–4077. [PubMed: 8382689]

34. Sokolovsky M. Porcine carboxypeptidase B. Nitration of the functional tyrosyl residue with tetranitromethane. Eur. J. Biochem 1972;25:267–273. [PubMed: 5064743]

35. El-Remessy AB, Al-Shabrawey M, Platt DH, Bartoli M, Behzadian MA, Ghaly N, Tsai N, Motamed K, Caldwell RB. Peroxynitrite mediates VEGF's angiogenic signal and function *via* a nitration-independent mechanism in endothelial cells. FASEB J 2007;21:2528–2539. [PubMed: 17384142]

36. Wolkow PP. Involvement and dual effects of nitric oxide in septic shock. Inflamm. Res 1998;47:152–166. [PubMed: 9628258]

37. Abdelmagid SA, Too CKL. Prolactin and estrogen up-regulate carboxypeptidase-D to promote nitric oxide production and survival of MCF-7 breast cancer cells. Endocrinology 2008;149:4821–4828. [PubMed: 18535109]

38. Radi R. Nitric oxide, oxidants, and protein tyrosine nitration. P. Natl. Acad. Sci. USA 2004;101:4003–4008.

39. Schopfer FJ, Baker PRS, Freeman BA. NO-dependent protein nitration: a cell signaling event or an oxidative inflammatory response? Trends Biochem. Sci 2003;28:646–654. [PubMed: 14659696]

40. Vendrell J, Querol E, Aviles FX. Metallocarboxypeptidases and their protein inhibitors. Structure, function and biomedical properties. Biochim. Biophys. Acta 2000;1477:284–298. [PubMed: 10708864]

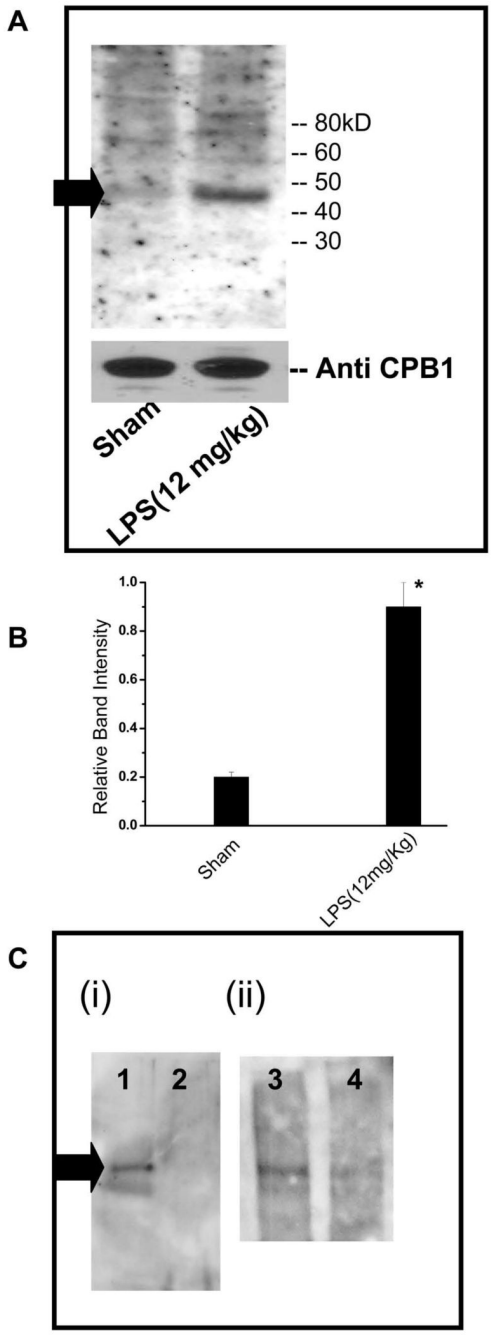

Fig. 1.

Immunoblotting of immunoprecipitated CPB1 from spleen tissue homogenates with anti-nitrotyrosine antibody. A) Spleen tissue proteins were isolated from control and LPS-treated mice and then immunoprecipitated with anti-CPB1 antibody and immunoblotted with anti-nitrotyrosine antibody. A 47 kD band corresponding to CPB1 is shown by a black arrow. Equal loading was confirmed using a direct ELISA of CPB1 present in the immunoprecipitate. The CPB1 band density was compared with nitrotyrosine band density for normalization. B) Densitometric analysis of normalized bad densities against anti-CPB1 immunoblots. * $P<0.05$ when compared to sham. Similar results were obtained in three independent experiments. C) In a control experiment the specificity of CPB1 tyrosine nitration was confirmed by pre-

absorbing the anti-CPB1 antiserum with recombinant mouse CPB1 (i, Lanes 2 and 4), bovine serum albumin (i, lane 1) and normal rabbit serum (ii, Lane 3)

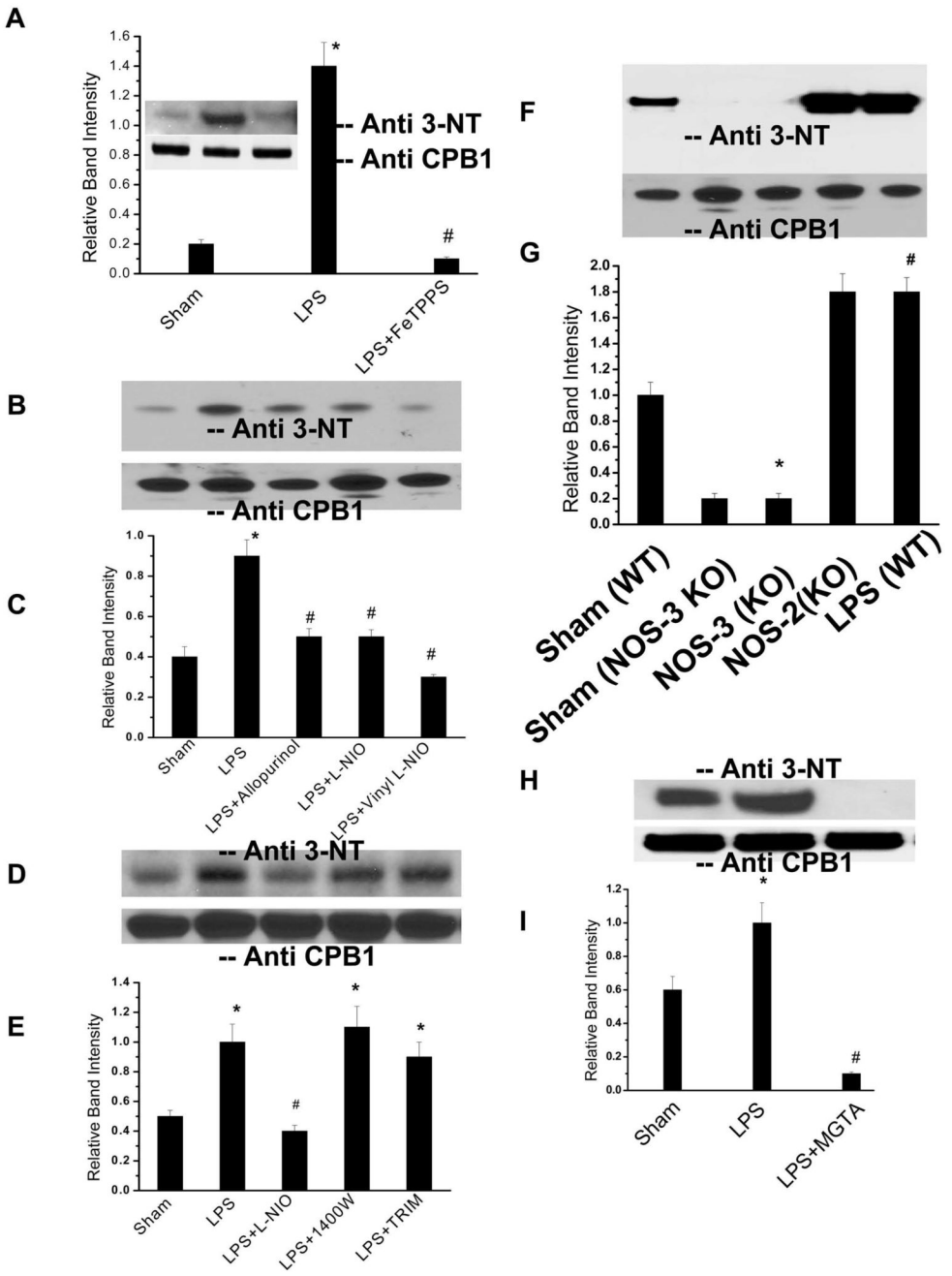

Fig. 2.

CPB1 tyrosine nitration is a result of peroxynitrite formation by dual action of NOS-3 and XO. A) Spleen proteins from sham-, LPS- and LPS+FeTPPS (Peroxynitrite decomposition catalyst)-treated mice were immunoprecipitated with anti-CPB1 antibody and were separated by SDS-PAGE and electroblotted on a nitrocellulose membrane. Western blot analysis was performed using an antibody specific to 3-nitrotyrosine (Inset). The bar chart shows the band intensity of the immunoreactive proteins. B). Spleen proteins from sham-, LPS-= LPS+L-NIO-, and LPS + Vinyl-L-NIO-treated mice (relatively specific NOS-3 inhibitors) and LPS + allopurinol-treated mice (XO specific inhibitor) were immunoprecipitated with anti-CPB1 antibody and were separated by SDS-PAGE and electroblotted on a nitrocellulose membrane.

Western blot analysis was performed using an antibody specific to 3-nitrotyrosine. C). A graphical representation of the band intensities of immunoreactive proteins. Equal loading was confirmed using a direct ELISA of CPB1 present in the immunoprecipitate. The CPB1 band density was compared with nitrotyrosine band density for normalization. * $P<0.05$ when compared to sham; # $P<0.05$ when compared to LPS (12 mg/kg)-treated mice. D) Spleen proteins from sham, LPS, LPS+L-NIO, LPS + 1400W (NOS-2 inhibitor) and LPS+TRIM (NOS-1 inhibitor)-treated mice were immunoprecipitated with anti-CPB1 antibody and were separated by SDS-PAGE and electroblotted on a nitrocellulose membrane. Western blot analysis was performed using an antibody specific to 3-nitrotyrosine. E) A graphical representation of the band intensities of immunoreactive proteins is also provided. Equal loading was confirmed using a direct ELISA of CPB1 present in the immunoprecipitate. The CPB1 band density was compared with nitrotyrosine band density for normalization. * $P<0.05$ when compared to sham; # $P<0.05$ when compared to LPS (12 mg/kg)-treated mice. F) Spleen proteins from sham- and LPS-treated wild type(WT) and NOS-3 knockout LPS (NOS-3 K/O) mice were immunoprecipitated with anti-CPB1 antibody and were separated by SDS-PAGE and electroblotted on a nitrocellulose membrane. Western blot analysis was performed using an antibody specific to 3-nitrotyrosine. G) A graphical representation of the band intensities of immunoreactive proteins. Equal loading was confirmed using a direct ELISA of CPB1 present in the immunoprecipitate. The CPB1 band density was compared with nitrotyrosine band density for normalization. * $P<0.05$ when compared to sham of NOS-3 KO; # $P<0.05$ when compared to sham-treated wild type mice. H) Spleen proteins from sham-, LPS- and LPS + MGTA- (CPB inhibitor that binds to the catalytic site) treated mice were immunoprecipitated with an anti-CPB1 antibody and were separated by SDS-PAGE and electroblotted on a nitrocellulose membrane. Western blot analysis was performed using an antibody specific to 3-nitrotyrosine. I) A graphical representation of the band intensities of immunoreactive proteins. Equal loading was confirmed using a direct ELISA of CPB1 present in the immunoprecipitate. The CPB1 band density was compared with nitrotyrosine band density for normalization. * $P<0.05$ when compared to sham; # $P<0.05$ when compared to LPS (12 mg/kg)-treated mice.

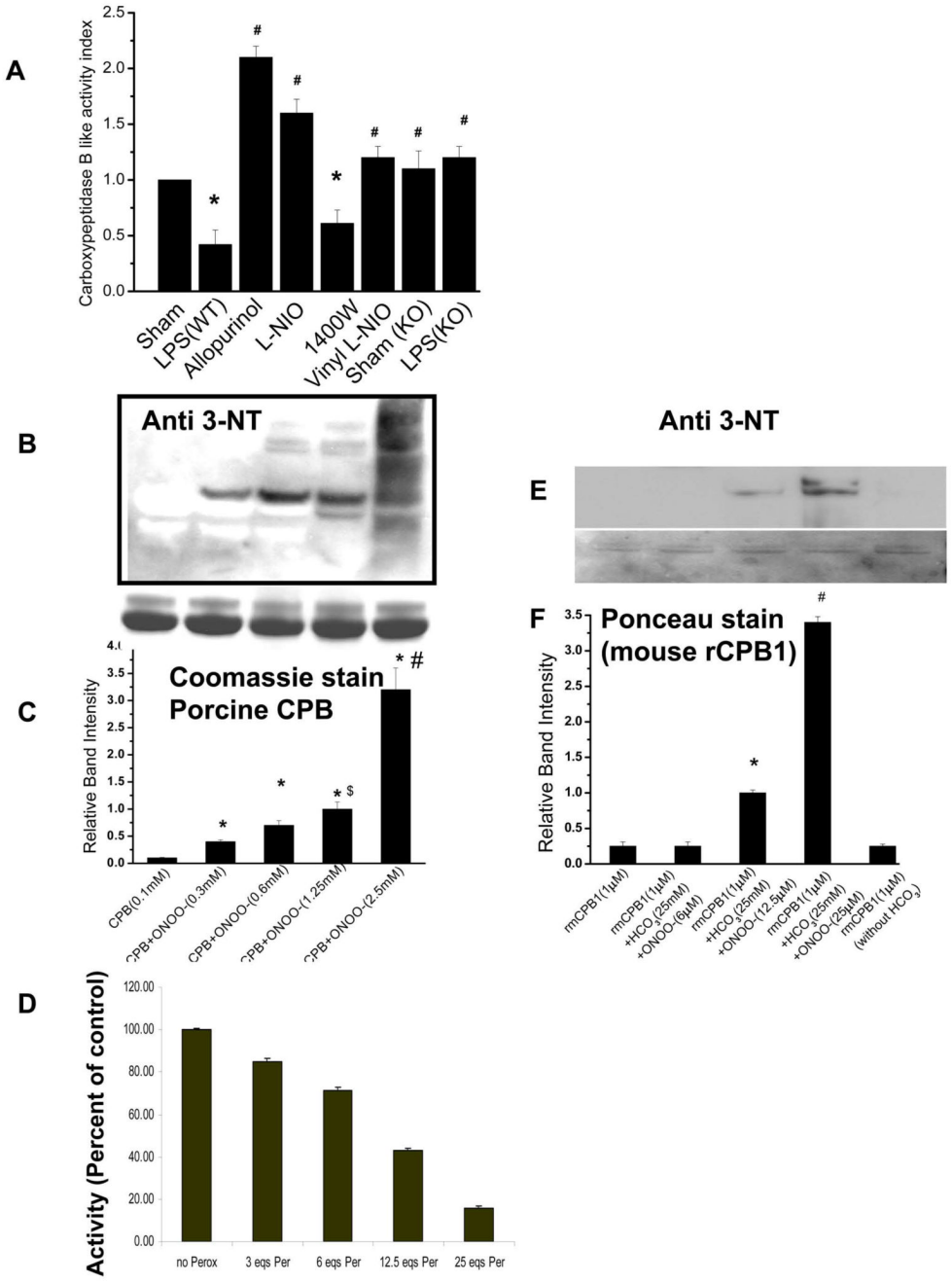

Fig. 3.

Peroxynitrite mediated tyrosine nitration inactivates CPB1 in the septic spleen and *in vitro*. A) CPB1 activity in spleen tissue homogenates from LPS, LPS + allopurinol, LPS + L-NIO, 1400W, LPS + Vinyl-L-NIO, and NOS-3 knockout mice was measured using an Actichrome TAFI Activity Kit with slight modifications, and activity indices were calculated using sham-treated values (Activity Index=Treated activity/sham activity). B). Tyrosine nitration mediated by peroxynitrite as a function of loss of activity of CPB. Porcine CPB (100 μM) was incubated with different concentrations of peroxynitrite. Samples were separated by SDS-PAGE, and the proteins were electroblotted on a nitrocellulose membrane. The blotted proteins were probed for 3-nitrotyrosine immunoreactivity using a 3-nitrotyrosine antibody. C) A graphical

representation of the band intensities of immunoreactive proteins. Equal loading was confirmed using Coommassie stained bands on the SDS PAGE gel. Furthermore, the CPB1 band density of the western with anti-CPB antibody was compared with nitrotyrosine band density for normalization. * P<0.05 when compared to the CPB only group; $P<0.05 when compared to the CPB+$ONOO^-$(0.6mM) group; #P<0.001 when compared to the CPB+ONOO-(1.25mM) group. D) Percentage activity of CPB as a function of 0, 3, 6, 12.5 and 25 molar equivalents of peroxynitrite. E). Mouse recombinant CPB1 (1 μM) was incubated with different concentrations of peroxynitrite. Samples were separated by SDS-PAGE and the proteins were electroblotted on a nitrocellulose membrane. The blotted proteins were probed for 3-nitrotyrosine immunoreactivity using a 3-nitrotyrosine antibody. F.) A graphical representation of the band intensities of immunoreactive proteins. Equal loading was confirmed using Ponceau stained bands on the nitrocellulose membrane. Furthermore, the CPB1 band density of the western with the anti-CPB1 antibody was compared with the nitrotyrosine band density for normalization. * P<0.05 when compared to the recombinant mouse CPB1 only group; #P<0.001 when compared to the CPB+ONOO-(25μM) group.

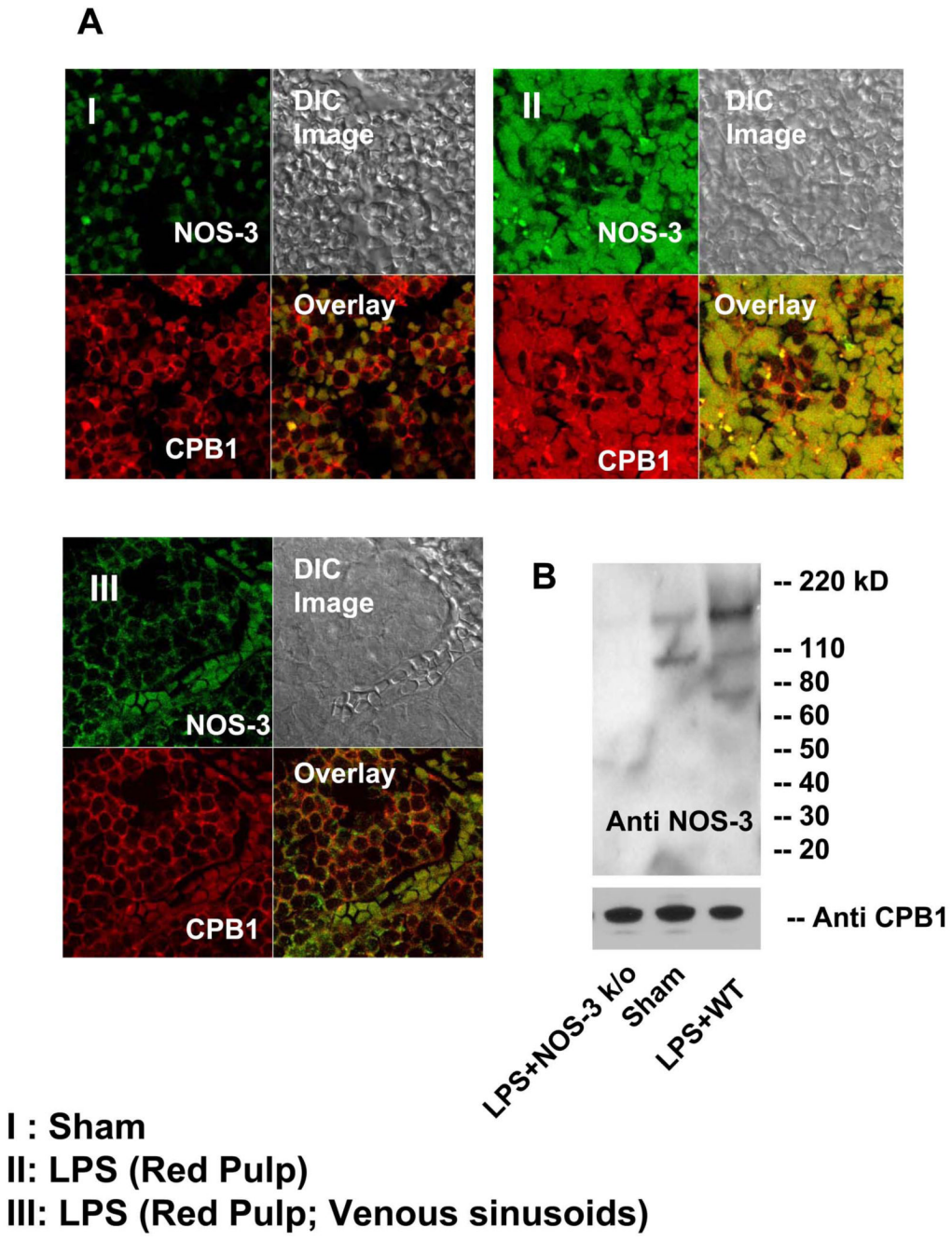

Fig. 4.

NOS-3 co-localization and protein complex formation with CPB1 contribute to its tyrosine nitration. A Blocks I, II, and III represent confocal imaging of spleen sections from sham- and LPS=-treated mice. The sections are focused on the splenic red pulp from the regions surrounding the venous sinusoids. Block III focuses on specific sinus lining cells of the red pulp. Each block represents staining in red (CPB1), green (NOS-3) and yellow (co-localized regions). C.) Spleen proteins from NOS-3 knockout- (negative control), sham- and LPS- (WT) treated mice were immunoprecipitated with anti-CPB1 antibody and were separated by SDS-PAGE and electroblotted on a nitrocellulose membrane. Western blot analysis was performed using a monoclonal antibody specific to mouse NOS-3.

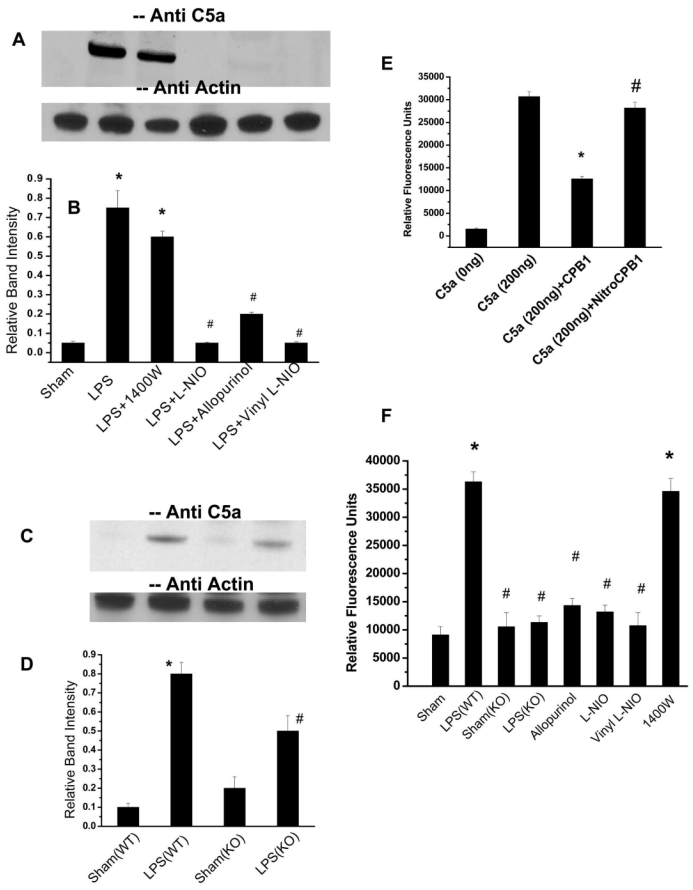

Fig. 5.

CPB1 tyrosine nitration results in C5a accumulation in the mouse spleen following LPS administration. A) Spleen proteins from sham, LPS, LPS + NOS-2 inhibitor 1400W, LPS + L-NIO, LPS + Vinyl-L-NIO (relatively specific NOS-3 inhibitors), and LPS + Allopurinol (XO inhibitor) were separated by SDS-PAGE and electroblotted on a nitrocellulose membrane. Western blot analysis was performed using an antibody specific to C5a. B) A bar graph represents the normalized relative band intensities of the western analysis of the proteins immunoreactive to C5a antibody. C) Spleen proteins from sham (wild type), LPS (wild type), sham (NOS-3 knockout) and LPS (NOS-3 knockout) were separated by SDS-PAGE and electroblotted on a nitrocellulose membrane. Western blot analysis was performed using an antibody specific to C5a. D) A bar graph represents the normalized relative band intensities of the western analysis of the proteins immunoreactive to C5a antibody.* P<0.05 when compared to the sham-treated of wild type mice; #P<0.05 when compared to the sham-treated of knockout mice. E) Chemotaxis of HL 60 cells in response to recombinant C5a. Also, recombinant C5a was incubated with both mouse recombinant CPB1 and nitro-CPB1 to assess the effect of nitration of CPB1 on C5a-induced chemotaxis. * P<0.05 when compared to rC5a alone; #P<0.05 when compared to rC5a + mouse rCPB1. F) Chemotaxis of HL-60 cells in response to immunoprecipitated C5a from LPS-treated (wild type), XO inhibitor-treated, NOS-3 inhibitors treated, NOS-2 inhibitor-treated and LPS-treated knockout mice spleen tissue homogenates was measured in terms of relative fluorescent intensity by a CytoselectTM 96 well cell migration assay following the manufacturer's protocol. . * P<0.05 when compared to sham-treated mice alone; #P<0.05 when compared to LPS-treated wild type mice.

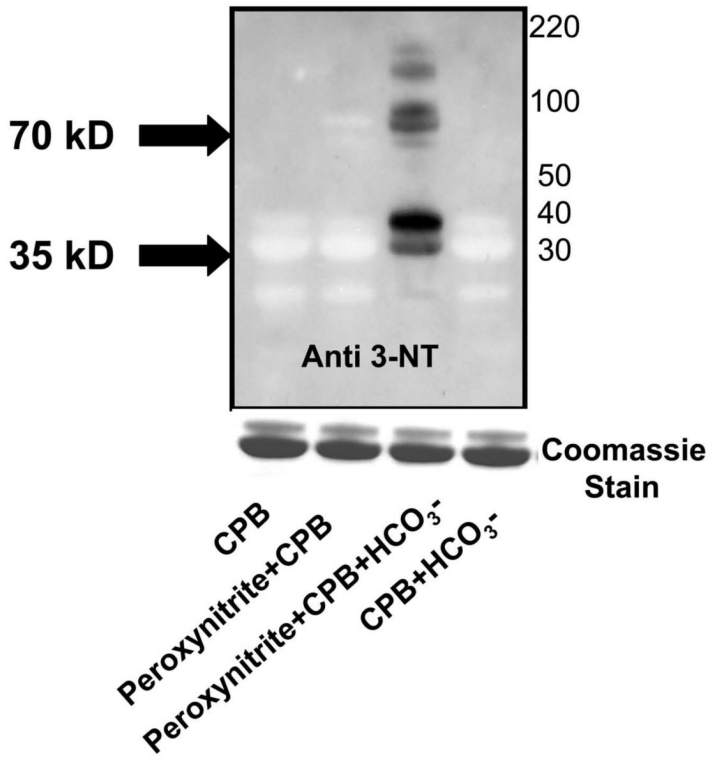

Fig. 6.

Role of carbonate radical formation in CPB tyrosine nitration. CPB (100μM) was incubated with 300 μM of peroxynitrite in the absence or in the presence of 25 mM sodium bicarbonate. The protein was then separated by SDS-PAGE and electroblotted on a nitrocellulose membrane. Western blot analysis was performed using an antibody specific to 3-nitrotyrosine. Coommassie stain of the protein on SDS-PAGE gel is included as a loading control. The western analysis is a representative of three independent experiments.

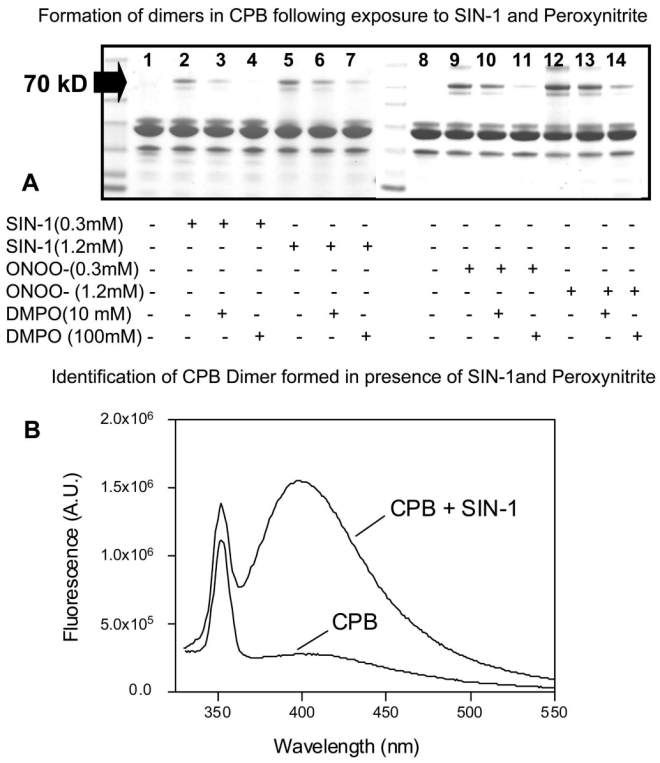

Fig. 7.

Formation of dityrosine dimer as a footprint of tyrosine radical formation on CPB by peroxynitrite. A) CPB (0.1 mM) was incubated with different concentrations of SIN-1 and peroxynitrite in the presence or absence of DMPO. The reaction mixture was then separated by SDS-PAGE and stained with Coommassie Blue. B) CPB (0.1 mM) was incubated with SIN-1 (0.3mM) for 1 h. The reaction mixture was then checked for an increase in fluorescence at 410 nm, characteristic of dityrosine dimer formation. The Coomassie Blue- stained gel photograph and the dityrosine dimer detection by fluorescence are representative of a total of three experiments.

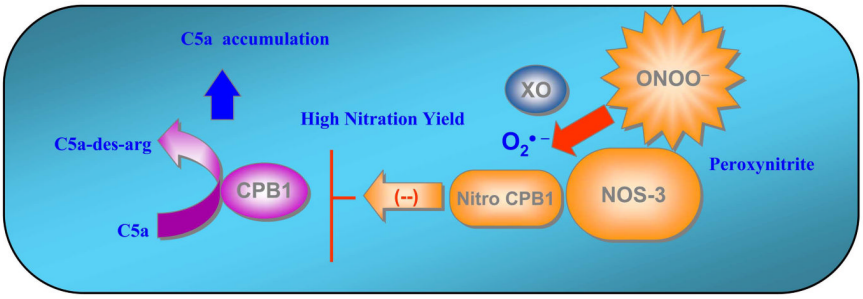

Fig. 8.

Tyrosine nitration of CPB1 in the sinus lining cells of the spleen. Proximal association and binding of CPB1 and NOS-3 possibly resulted in higher nitration yield in the local milieu, leading to loss of CPB1 activity. This would possibly lead to accumulation of inflammatory mediators like C5a in the spleen, thus amplifying the systemic inflammatory response and altering immune pathology.

Altered patho-physiology in septic spleen following NOS-3 and CPB1 coupling

Table.I

Summary of identified peptides originating from proteolytic digestion of CPB and nitrated tyrosine residues

Summary of identified peptides originating from proteolytic digestion of porcine CPB. Tryptic and chymotryptic digestions of untreated CPB and CPB reacted with peroxynitrite were subjected to reverse phase HPLC. Absorbance at 365 nm was used to monitor the elution of the nitrated peptide fragment. The fractions showing intense signal at 365 nm were collected and further characterized by tandem mass spectrometry.

* PROTEASE	ELUTION TIME	POSITION OF YNO2	SEQUENCE
Try	45.6	210	(Y) S<u>Y</u>DYKLPENNAELNNLA(K)
Try	48.3	248	(K) YTYGPGATTI<u>Y</u>PAAGGSDDWAYDQGIK(Y)
Try	52.6	92	(R) EAVLT<u>Y</u>GYESHMTEFLN(K)
Try	58.79	277	(R) <u>Y</u>GFILPESQIQATCEETMLAIK(Y)
Try	61.4	277	(R) <u>Y</u>GFILPESQIQATCEETMLAI(K)
Chy	30.9	277	(F) ELRDKGR<u>Y</u>(G)
Chy	40.84	198	(Y) LTIHS<u>Y</u>(S)
Chy	41.43	210	(Y) S<u>Y</u>DYKLPENNAELNNL(A)
Chy	41.77	92	(Y) G<u>Y</u>ESHMTEF(L)
Chy	41.77	248	(T) I<u>Y</u>PAAGGSDDW(A)
Chy	41.83	92	(Y) G<u>Y</u>ESHMTEF(L)
Chy	42.06	248	(T) I<u>Y</u>PAAGGSDDW(A)

* Try: Trypsin, Chy: Chymotrypsin